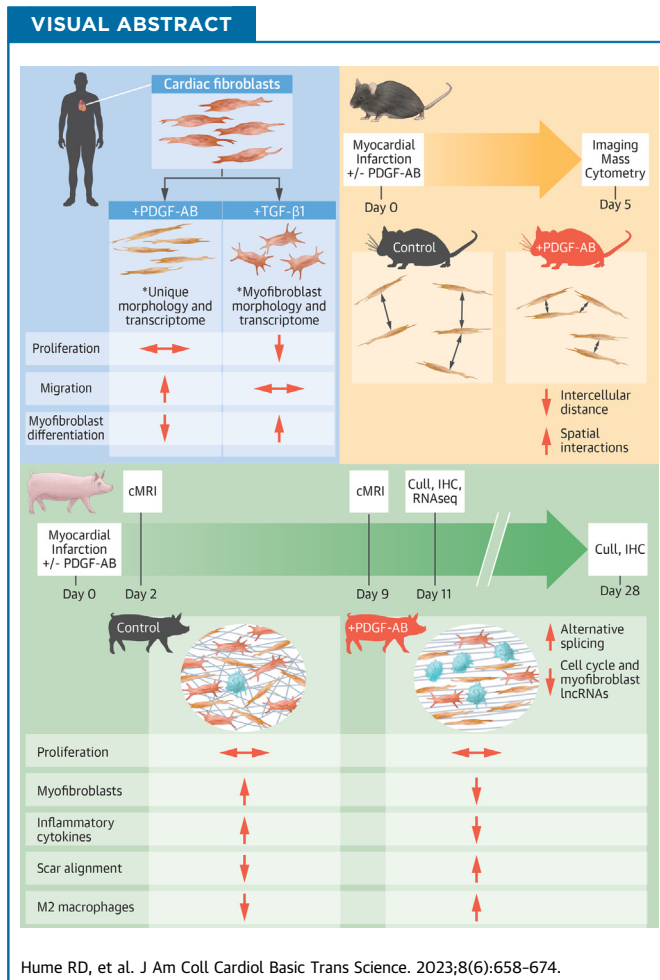


ORIGINAL RESEARCH - PRECLINICAL

# PDGF-AB Reduces Myofibroblast Differentiation Without Increasing Proliferation After Myocardial Infarction



Robert D. Hume, PhD,<sup>a,b</sup> Tejas Deshmukh, MBBS, MCLINTR,<sup>a,b,c</sup> Tram Doan, PhD,<sup>d</sup> Woo Jun Shim, PhD,<sup>e</sup> Shaan Kanagalingam, BSc,<sup>a</sup> Vikram Tallapragada, PhD,<sup>f</sup> Fairooj Rashid, MSc,<sup>a,b</sup> Maria Marcuello, PhD,<sup>g</sup> Daniel Blessing, PhD,<sup>g</sup> Dinesh Selvakumar, MBBS,<sup>a,b,c</sup> Kalyan Raguram, BMED,<sup>a,b</sup> Faraz Pathan, MBBS, PhD,<sup>h,i</sup> Dinny Graham, PhD,<sup>d,j,k</sup> Samir Ounzain, PhD,<sup>g</sup> Eddy Kizana, PhD,<sup>a,b,c</sup> Richard P. Harvey, PhD,<sup>f,l,m,n</sup> Nathan J. Palpant, PhD,<sup>e</sup> James J.H. Chong, MBBS, PhD<sup>a,b,c</sup>



## SUMMARY

After myocardial infarction (MI), fibroblasts progress from proliferative to myofibroblast states, resulting in fibrosis. Platelet-derived growth factors (PDGFs) are reported to induce fibroblast proliferation, myofibroblast differentiation, and fibrosis. However, we have previously shown that PDGFs improve heart function post-MI without increasing fibrosis. We treated human cardiac fibroblasts with PDGF isoforms then performed RNA sequencing to show that PDGFs reduced cardiac fibroblasts myofibroblast differentiation and downregulated cell cycle pathways. Using mouse/pig MI models, we reveal that PDGF-AB infusion increases cell-cell interactions, reduces myofibroblast differentiation, does not affect proliferation, and accelerates scar formation. RNA sequencing of pig hearts after MI showed that PDGF-AB reduces inflammatory cytokines and alters both transcript variants and long noncoding RNA expression in cell cycle pathways. We propose that PDGF-AB could be used therapeutically to manipulate post-MI scar maturation with subsequent beneficial effects on cardiac function. (J Am Coll Cardiol Basic Trans Science 2023;8:658-674) © 2023 The Authors. Published by Elsevier on behalf of the American College of Cardiology Foundation. This is an open access article under the CC BY-NC-ND license (<http://creativecommons.org/licenses/by-nc-nd/4.0/>).

Myocardial infarction (MI) affects millions of people every year and is a significant burden on global health care systems.<sup>1</sup> This event is predominantly caused by atherosclerotic plaque rupture, formation of thrombi, and subsequent occlusion in 1 or more coronary arteries.<sup>2</sup> Ischemia distal to the occluded vessel then causes necrosis and cardiomyocyte (CM) cell death. This loss of viable CMs causes decreased heart function and potential heart failure. Following clearing of necrotic CMs, both resident and migratory fibroblasts proliferate in the infarct zone (IZ) and border zone (BZ).<sup>3</sup> At this stage, fibroblast fate shifts from a leukocyte-recruiting antimigratory phenotype (day 1) to a proliferative proangiogenic profibrotic phenotype (day 3), accompanied by synthesis of a preliminary fibronectin-rich replacement extracellular matrix (ECM).<sup>4,5</sup> After this proliferative phase, fibroblasts synthesize a more mature ECM comprising increased collagens and other proteins, including periostin and tenascin.<sup>5</sup> Fibroblasts then differentiate into  $\alpha$ -smooth muscle actin (SMA) expressing myofibroblasts.<sup>6</sup> These myofibroblasts possess superior fibrotic potential and are responsible for the synthesis of a lysyl oxidase (LOX) cross-linked collagen-I-rich replacement scar.<sup>3</sup> Concurrent with these fibroblast fate transitions is a complex immune response, initiated post-MI, with an inflammatory phase.<sup>3</sup> If this inflammatory phase is prolonged, continued production of cytokines can cause adverse remodeling, decreased

heart function, and potential heart failure.<sup>7,8</sup> Conversely, reduced levels of these proinflammatory cytokines can have reparative effects.<sup>9,10</sup>

Platelet-derived growth factors (PDGFs) are dimeric glycoproteins, commonly reported as promigratory potent mitogens for cells of a mesenchymal origin, such as fibroblasts.<sup>11</sup> They are secreted as a disulfide-linked homodimer of 2 A subunits (PDGF-AA), 2 B subunits (PDGF-BB), or heterodimers of subunits A and B (PDGF-AB).<sup>12</sup> Tyrosine kinase receptors to these ligands are comprised of 2 monomers, PDGFR $\alpha$  and PDGFR $\beta$ , which form homodimers PDGFR $\alpha\alpha$  (binds PDGF-AA, -AB, and -BB), PDGFR $\beta\beta$  (binds PDGF-BB), or the heterodimer PDGFR $\alpha\beta$  (binds PDGF-AB and -BB).<sup>12</sup>

Differentiation of fibroblasts to myofibroblasts is a hallmark of increased tissue fibrosis and occurs during scar maturation after MI.<sup>6</sup> The literature reports that PDGFs increase fibroblast-myofibroblast differentiation and can therefore contribute to excessive fibrosis.<sup>13-15</sup> However, our previous studies have shown that introducing exogenous PDGFs in small and large animal models of MI does not increase scar size, as would be predicted if increased fibrosis were to occur.<sup>16-18</sup> Specifically, in

## ABBREVIATIONS AND ACRONYMS

- AURKB** = human gene encoding aurora B kinase
- BZ** = border zone
- cFib** = human cardiac fibroblasts
- CCNT1** = human gene encoding cyclin-T1
- CM** = cardiomyocyte
- cMRI** = cardiac magnetic resonance
- col1 $\alpha$ 1** = collagen type-I- $\alpha$ -1
- col1 $\alpha$ 2** = collagen type-I- $\alpha$ -2
- cSC** = cardiac stromal cell
- DAVID** = Database for Annotation, Visualization and Integrated Discovery
- DE** = differential expression
- DTU** = differential transcript usage
- ECM** = extracellular matrix
- FNI** = human gene encoding fibronectin-1
- GSEA** = gene set enrichment analysis
- IHC** = immunohistochemistry
- IMC** = imaging mass cytometry
- IL** = interleukin
- IZ** = infarct zone
- lncRNA** = long noncoding RNA
- LOX** = lysyl oxidase
- MBLNI** = muscleblind-like 1
- PCA** = principal component analysis
- PDGF** = platelet derived growth factor
- PDGFR** = platelet-derived growth factor receptor
- POSTN** = human gene encoding periostin
- RNAseq** = ribonucleic acid sequencing
- RZ** = remote zone
- SMA** = smooth muscle actin
- SRF** = serum response factor
- TGF** = transforming growth factor
- TNC** = tenascin-C

From the <sup>a</sup>Centre for Heart Research, Westmead Institute for Medical Research, Westmead, New South Wales, Australia; <sup>b</sup>Sydney Medical School, University of Sydney, New South Wales, Australia; <sup>c</sup>Department of Cardiology, Westmead Hospital, Westmead, New South Wales, Australia; <sup>d</sup>Centre for Cancer Research, Westmead Institute for Medical Research, Westmead, New South Wales, Australia; <sup>e</sup>Institute for Molecular Bioscience, University of Queensland, St Lucia, Queensland, Australia; <sup>f</sup>Victor Chang

our previous rodent studies, we observed a reduced scar size with improved heart function.<sup>17</sup> In our previous pig studies, there was no difference in post-MI scar size but rather increased collagen scar anisotropy (directionality), increased angiogenesis, improved left ventricular ejection fraction (LVEF), and improved myocardial contractility.<sup>16</sup> This presents an opportunity to investigate how PDGFs might impact fibroblast proliferation and myofibroblast differentiation without increasing overall fibrosis after MI.

In the present study, we sought to shed light on the impact of PDGFs on the infarcted heart. We first interrogated the effects of PDGF isoforms on human cardiac fibroblast-myofibroblast differentiation. These data revealed unexpected findings and show that PDGF treatment yields a cardiac fibroblast phenotype unique from myofibroblasts capable of enhancing angiogenesis, cellular migration, and collagen synthesis. To understand PDGF effects in vivo, we then used a mouse model of MI with PDGF-AB systemic infusion and performed imaging mass cytometry (IMC) on treated and control hearts. This technique provides large-scale spatial data on single cell protein expression. We show specific effects of PDGF-AB treatment on unique cell populations with altered proportions and spatial interactions. For further translational relevance, we used a porcine model of MI with PDGF-AB systemic infusion.<sup>17</sup> This shows intriguing effects of PDGF-AB on pig fibroblast-myofibroblast differentiation, scar formation, and immune response. Finally, using paired-end RNA sequencing (RNAseq) combined with de novo library assembly, we improve upon current pig genome annotations and interrogate post-MI PDGF-AB effects on gene, transcript variant, and long noncoding RNA (lncRNA) expression.<sup>19</sup> Taken together, our results show the ability of exogenous PDGF-AB delivery to reduce myofibroblast differentiation and permit a reparative setting for accelerated scar maturation without overall increased fibrosis.

## METHODS

**STATISTICAL METHODS.** Data are presented using the mean  $\pm$  SD and compared using 1-way analysis of variance with Tukey's post hoc test for multiple pairwise comparisons. GraphPad Prism version 8.0 (GraphPad Software) was used for all column analyses excluding RNAseq.

For RNAseq data, DESeq2 R library was used for differential gene expression (DE) analysis (RStudio, PBC). Genes were identified as having significant DE if the gene was either up- or downregulated compared to the control (absolute log<sub>2</sub>-fold change  $\geq 0.5$  or  $\leq -0.5$ ), and this difference was statistically significant (Benjamini and Hochberg adjusted  $P \leq 0.05$ ).

For principal component analysis (PCA) analyses of RNAseq data, genes with total read counts across all samples  $< 10$  were considered not expressed and removed from downstream analysis. Raw read counts were transformed using variance stabilization transformation method (vst function) from the DESeq2 package, which resulted in approximated variance stabilized, log<sub>2</sub> transformed expression values. Batch effect correction was also performed using the removeBatchEffect function from the limma package. The vst-transformed, batch effect-corrected expression values were used as input for principal component analysis. Principal component analysis and visualization of the samples in the first 2 principal components were performed using the plotPCA function of the DESeq2 package.

For RNAseq heatmap hierarchical clustering, differentially expressed genes with a log<sub>2</sub>-fold change of  $\geq 0.5$  or  $\leq -0.5$  and an adjusted  $P \leq 0.05$  were clustered by rows using Euclidian distance as a metric and an average linkage method, with the online resource Morpheus (Broad Institute).<sup>20</sup> Volcano plots of differentially regulated genes were generated using the EnhancedVolcano RStudio package with a log<sub>2</sub>-fold change cutoff of  $\geq 0.5$  or  $\leq -0.5$  and an adjusted  $P \leq 0.05$ . Full methods can be found in the [Supplemental Appendix](#).

---

Cardiac Research Institute, Darlinghurst, New South Wales, Australia; <sup>g</sup>HAYA Therapeutics, Lausanne, Switzerland; <sup>h</sup>Nepean Clinical School of Medicine, Charles Perkin Centre Nepean, University of Sydney, Kingswood, New South Wales, Australia; <sup>i</sup>Department of Cardiology, Nepean Hospital, Kingswood, New South Wales, Australia; <sup>j</sup>Westmead Breast Cancer Institute, Westmead, New South Wales, Australia; <sup>k</sup>Westmead Clinical School, University of Sydney, New South Wales, Australia; <sup>l</sup>St Vincent's Clinical School, University of New South Wales-Sydney, Kensington, New South Wales, Australia; <sup>m</sup>Melbourne Brain Centre, University of Melbourne, Victoria, Australia; and the <sup>n</sup>School of Biotechnology and Biomolecular Science, University of New South Wales-Sydney, Kensington, New South Wales, Australia.

The authors attest they are in compliance with human studies committees and animal welfare regulations of the authors' institutions and Food and Drug Administration guidelines, including patient consent where appropriate. For more information, visit the [Author Center](#).

## RESULTS

### PDGFs REDUCE FIBROBLAST-MYOFIBROBLAST DIFFERENTIATION IN HUMAN CARDIAC FIBROBLASTS.

Previous studies report that PDGFs increase fibroblast-myofibroblast differentiation.<sup>13-15</sup> To understand if this occurs in human cardiac fibroblasts (cFib) we isolated cFib from human left ventricular cardiac tissue obtained from multiple donors with no known comorbidities. After this, we treated each cFib donor-derived cell line with either PDGF-AB, transforming growth factor (TGF)- $\beta$ 1, or a combination of the 2 growth factors. TGF- $\beta$ 1 is known to induce fibroblast-myofibroblast differentiation in vitro and in vivo following MI.<sup>21</sup> Therefore, it was used as a control for myofibroblast differentiation. As expected, TGF- $\beta$ 1-treated cFib showed typical myofibroblast “wide/flat” morphology and increased myofibroblast marker  $\alpha$ -SMA expression (Figures 1A to 1C, Videos 1 to 3). Surprisingly, PDGF-AB-treated cFib progressed from a wide/flat morphology to a “spindle-shaped” morphology (Videos 1 to 3) with reduced  $\alpha$ -SMA protein and reduced *ACTA2* (encoding  $\alpha$ -SMA) gene expression (Figures 1A to 1D). Therefore, PDGF-AB reduced cFib-myofibroblast differentiation. When both TGF- $\beta$ 1 and PDGF-AB were combined, an intermediary phenotype was observed (Figures 1A to 1D).

To discern whether these effects from the PDGF-AB were unique to this PDGF isoform, we treated multiple cFib donor-derived cell lines with PDGF-AA, PDGF-AB, and PDGF-BB isoforms  $\pm$  TGF- $\beta$ 1 and performed immunocytochemistry. Similar to PDGF-AB, both PDGF-AA- and PDGF-BB-treated cFib showed no increase in myofibroblast marker  $\alpha$ -SMA protein expression (Figure 1E).

We previously described a cardiac stromal cell (cSC) population capable of multilineage in vitro differentiation.<sup>22</sup> To understand whether PDGF isoforms also reduced myofibroblast differentiation in this population, we isolated human cSC from cFib and treated with PDGF isoforms. We found similar morphological change, reduced  $\alpha$ -SMA protein expression, and reduced *ACTA2* gene expression in response to PDGF-AB (Supplemental Figure 4). As with cFib, PDGF isoforms alone did not increase  $\alpha$ -SMA expression in cSC (Supplemental Figure 4). Together, these data suggest that PDGFs reduce cFib and cSC differentiation into myofibroblasts, cells that are integral to infarct scar formation and fibrosis. Knowing that PDGFs can target both populations to reduce myofibroblast differentiation helps elucidate

potential therapeutic effects and understand their specificity/targets.

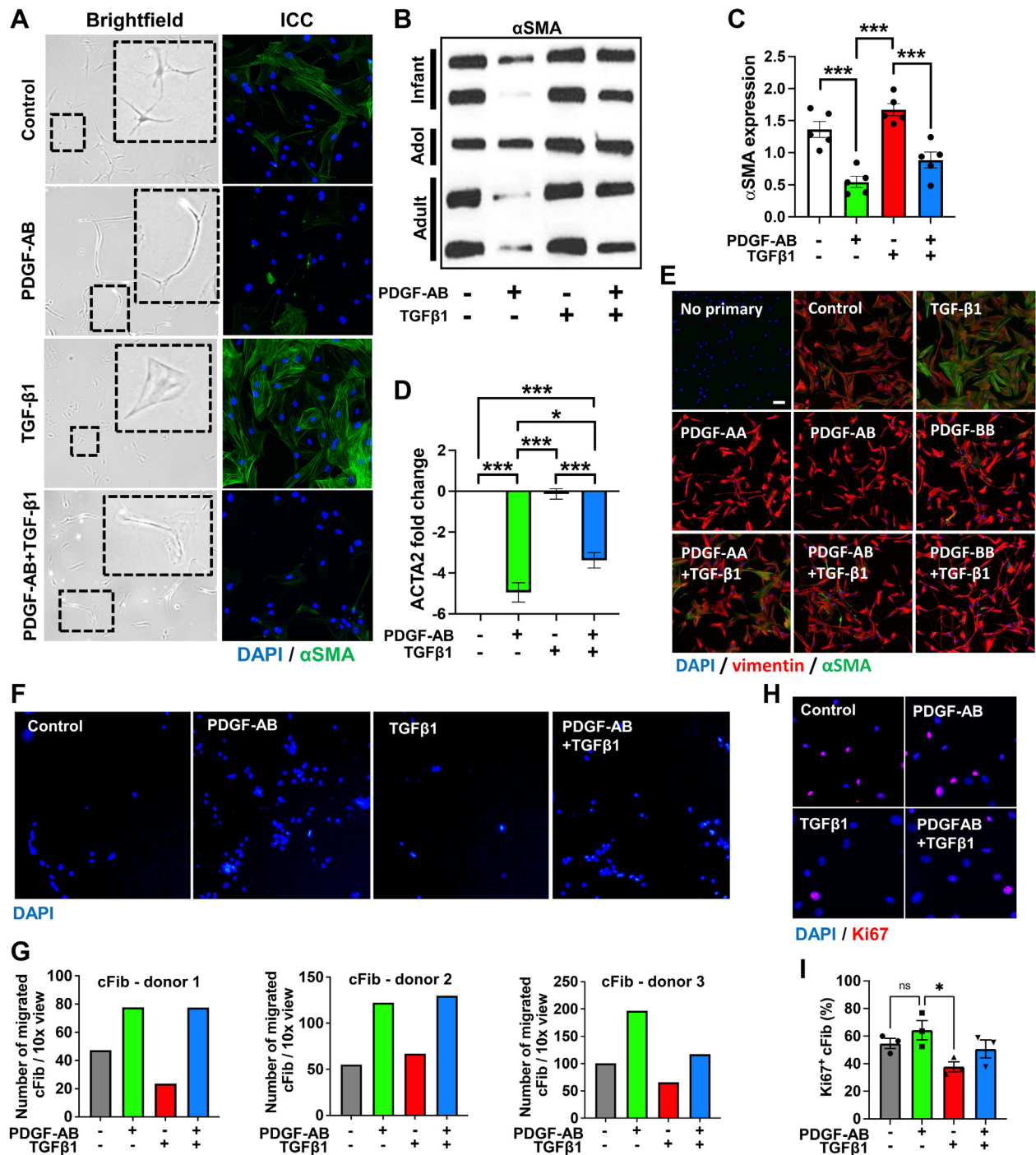
### PDGF-AB INCREASES cFib MIGRATION WITHOUT INCREASING PROLIFERATION.

Although it is reported that PDGFs increase the migration and proliferation of fibroblasts in vitro and in vivo within multiple organs, this has not been shown for cFib.<sup>11</sup> Therefore, we treated our donor-derived cFib cell lines with PDGF-AB in transwell migration assays. Despite significant biological differences, each individual donor-derived cFib cell line showed increased migration following PDGF-AB treatment compared to controls (Figures 1F and 1G). Live cell imaging also showed increased migration and cell-cell interactions in PDGF-AB-treated samples (Videos 1 to 3).

To investigate proliferation, we immunostained treated cFib with the proliferation marker Ki67. Although Ki67 expression was reduced in TGF $\beta$ 1-treated cFib as previously reported for lung myofibroblasts, there was no significant difference in PDGF-AB-treated cFib over untreated controls (Figures 1H and 1I).<sup>23</sup> Therefore, despite the potential for PDGFs to act as a fibroblast mitogen in a number of contexts, our data show that PDGF-AB treatment of donor-derived cFib increases migration without increasing proliferation.<sup>11</sup>

### PDGF-AB AND PDGF-BB HAVE SIMILAR EFFECTS ON cFib GENE EXPRESSION DISTINCT FROM PDGF-AA.

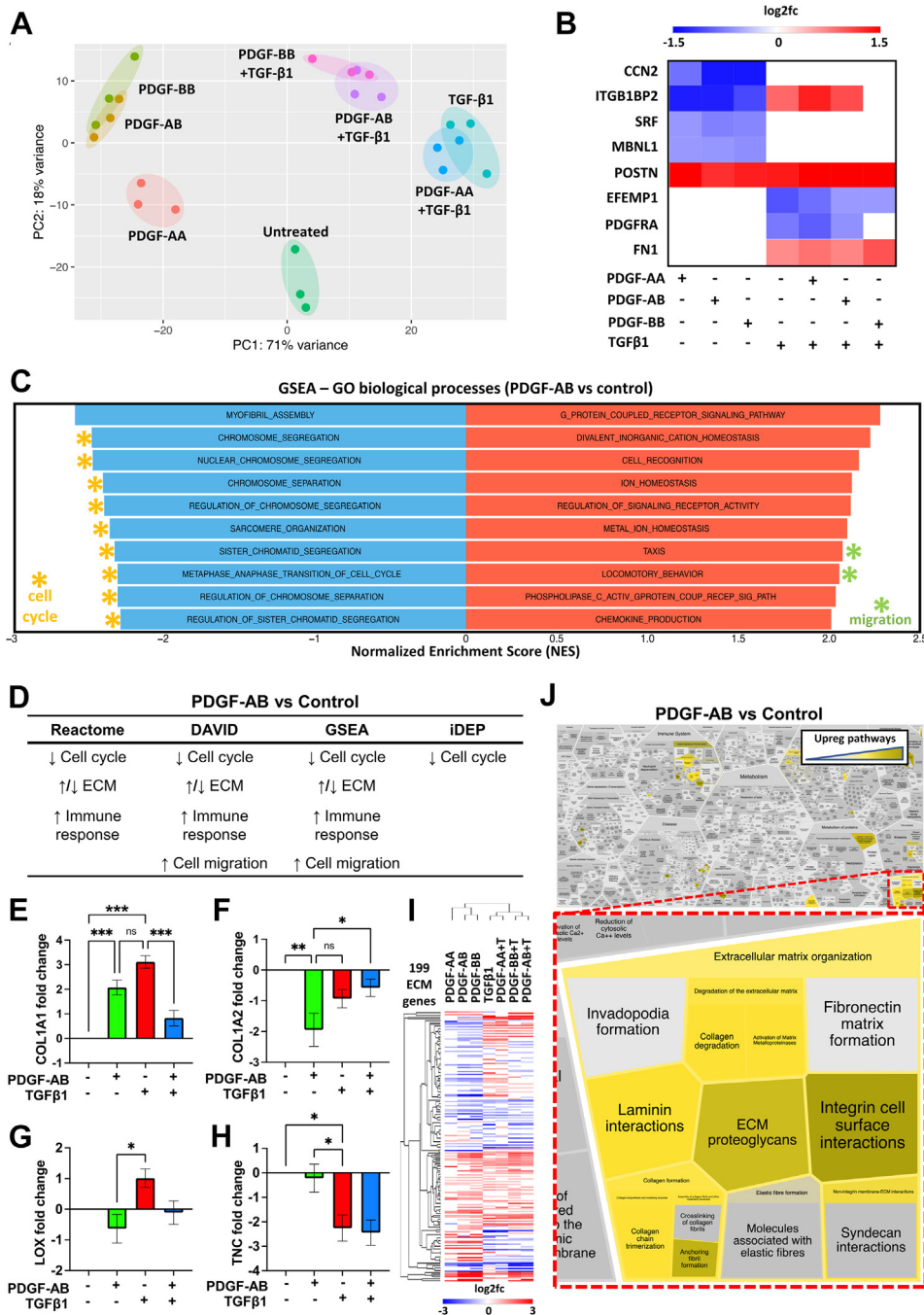
We next analyzed differences between PDGF isoforms on cFib using bulk RNAseq, PCA, heatmap hierarchical clustering, and volcano plot comparisons. No PDGF isoforms clustered with untreated controls, showing that they all exert effects on cFib gene expression (Figure 2A, Supplemental Figures 5A to 5D). However, these effects were weaker for PDGF-AA-treated cFib (Figure 2A, Supplemental Figures 5A to 5D). PDGF-AB and PDGF-BB samples clustered together and separately from PDGF-AA (Figure 2A, Supplemental Figures 5A to 5D), demonstrating similar effects on cFib gene expression distinct from PDGF-AA. Additionally, PDGF-AB + TGF- $\beta$ 1 and PDGF-BB + TGF- $\beta$ 1 samples also clustered together whereas PDGF-AA + TGF- $\beta$ 1 unexpectedly clustered with TGF $\beta$ 1 controls (Figure 2A, Supplemental Figures 5A to 5D). This suggests that during treatment with PDGF-AA + TGF $\beta$ 1, resultant cFib gene expression is driven by TGF- $\beta$ 1 whereas PDGF-AA has little effect (Supplemental Figures 5E and 5F). Additionally, PDGF-AB/PDGF-BB had an increased number of overlapping DE genes (823) compared to PDGF-AA/PDGF-AB (57) and PDGF-AA/PDGF-BB (31)

**FIGURE 1** PDGFs Reduce Fibroblast-Myofibroblast Differentiation and Increase Migration Without Increasing Proliferation of human cFib

Human cardiac fibroblasts (cFib) were treated with platelet-derived growth factor (PDGF) subunits AA, AB, or BB  $\pm$  transforming growth factor (TGF)- $\beta$ 1. **(A)** cFib were imaged using brightfield microscopy and immunostained with  $\alpha$ -smooth muscle actin (SMA) (green). **(B)** cFib Western blotting probed for  $\alpha$ SMA. **(C)** cFib Western blotting  $\alpha$ -SMA densitometry analysis. **(D)** cFib quantitative polymerase chain reaction (qPCR) for actin alpha 2, smooth muscle (ACTA2) fold change normalized to glyceraldehyde-3-phosphate dehydrogenase (GAPDH) ( $2^{-\Delta\Delta C_t}$ ). **(E)** cFib immunostained for vimentin (red) and  $\alpha$ -SMA (green). **(F)** cFib transwell assays showing 4',6-diamidino-2-phenylindole (DAPI)-stained migratory cells. **(G)** Analysis of transwell assays, each graph representing a different cFib donor-derived cell line. **(H)** cFib immunostaining for Ki67 (red) positive DAPI (blue). **(I)** Image analysis of proliferating (Ki67<sup>+</sup>) cFib. Statistical analyses were performed using a 1-way analysis of variance with a Tukey's multiple comparisons test. \* $P < 0.05$ . \*\*\* $P < 0.001$ . n.s. = not significant.



**FIGURE 2 PDGFs Reduce Myofibroblast and Cell Cycle Gene Expression and Increase Migration and ECM Gene Expression of cFib**



cFib were treated with PDGF-AA, PDGF-AB, or PDGF-BB ± TGFβ1 followed by RNA sequencing (RNAseq). **(A)** Principal component analysis (PCA). **(B)** Differential gene expression (DE) analysis heatmap of myofibroblast markers (scale bar = log<sub>2</sub>fold change). **(C)** Gene set enrichment analysis (GSEA) of PDGF-AB-treated samples showing the top and bottom 10 most effected gene sets. **(D)** Summary of RNAseq pathway analyses for PDGF-AB samples. **(E to H)** cFib qPCR for extracellular matrix (ECM) genes normalized to GAPDH ( $2^{-\Delta\Delta Ct}$ , n.s., \* $P < 0.05$ , \*\* $P < 0.01$ , \*\*\* $P < 0.001$ ). **(I)** Heatmap of cFib RNAseq ECM-related genes with hierarchical clustering (scale bar = log<sub>2</sub>fold change). **(J)** Reactome pathway analysis of PDGF-AB-treated cFib RNAseq gene expression showing upregulated pathways (yellow) highlighting ECM-related pathways (red inset). Abbreviations as in Figure 1.

(Supplemental Figure 5G). Together, these data show that PDGF-AB and PDGF-BB have an increased and similar effect on cFib as compared to PDGF-AA. Because PDGF-AA is only known to signal through PDGFR- $\alpha\alpha$ , we suggest that PDGF-AA-PDGFR- $\alpha\alpha$  signaling is less potent than PDGF-AB-PDGFR- $\alpha\alpha$ /PDGFR- $\alpha\beta$  or PDGF-BB-PDGFR- $\alpha\alpha$ /PDGFR- $\alpha\beta$ /PDGFR- $\beta\beta$  signaling in cFib.<sup>12</sup> These results also suggest that PDGF-AA has negligible effects in the presence of TGF- $\beta$ 1.

**PDGFs REDUCE MYOFIBROBLAST MARKER GENE EXPRESSION.** Using our cFib RNAseq dataset, we interrogated DE of known myofibroblast genes. Expectedly, we found that TGF $\beta$ 1 treatment upregulated *ITGB1BP2*,<sup>24</sup> periostin (*POSTN*),<sup>25,26</sup> and fibronectin-1 (*FN1*)<sup>26,27</sup> while downregulating *EFEMP1*<sup>28</sup> and *PDGFR- $\alpha$* .<sup>18,29</sup> (Figure 2B). Conversely, all PDGF isoforms had no effect or a converse effect on myofibroblast gene expression, excluding *POSTN*, an angiogenic<sup>30</sup> ECM protein (Figure 2B). Muscleblind-like 1 (*MBLN1*) protein stabilization of serum response factor (SRF) has recently been shown as necessary for TGF- $\beta$ 1-mediated myofibroblast differentiation and *MBLN1* deletion decreases myofibroblast density post-MI.<sup>31,32</sup> We found that all PDGF isoforms reduced *MBLN1* and *SRF* gene expression in cFib, further supporting our evidence of reduced myofibroblast transition during PDGF-treatment (Figure 2B).

Our previous studies in both small and large animal models have shown that PDGF-AB improves heart function post-MI.<sup>17,18</sup> For this reason and because our present data show similar effects of PDGF-AB and PDGF-BB, we shifted focus for the remainder of this study to the PDGF-AB isoform.

**PDGF-AB-TREATED cFib TRANSCRIPTOME PATHWAY ANALYSIS SHOWS INCREASED MIGRATION, REDUCED CELL CYCLE, IMMUNOMODULATION, AND UNIQUE ECM GENE EXPRESSION.** To further investigate how PDGF-AB effected cFib gene expression, we performed multiple pathway analyses of our cFib RNAseq dataset. Gene set enrichment analysis (GSEA) and the Database for Annotation, Visualization and Integrated Discovery (DAVID) showed upregulation of multiple migration-related (Figures 2C and 2D, Supplemental Figure 6A) and angiogenic (Supplemental Figure 6A) pathways following PDGF-AB treatment. DAVID, GSEA, integrated differential expression and pathway analysis, and Reactome pathway analyses of our cFib dataset all showed downregulation of multiple cell cycle pathways and increased immunomodulation after PDGF-AB treatment (Figures 2C and 2D, Supplemental Figure 6).

A major component of the post-MI scar is collagen type-I, which comprises a triple helix of 2 collagen type-I- $\alpha$ -1 (*col1 $\alpha$ 1*) and 1 collagen type-I- $\alpha$ -2 (*col1 $\alpha$ 2*) molecules.<sup>33</sup> During post-MI scar maturation, collagen type-I can undergo excessive LOX-mediated cross-linking associated with decreased heart function.<sup>34</sup> To interrogate PDGF-AB effects on the ECM, we first performed quantitative polymerase chain reaction (qPCR) on these target genes. Despite reduced myofibroblast differentiation, PDGF-AB-treated cFib had increased collagen type-I gene expression albeit with an altered *COL1A1:COL1A2* ratio and reduced LOX cross-linking (Figures 2E to 2G). Tenascin-C (TNC) is an ECM protein highly expressed at the end of the proliferative phase of MI repair (day 5). Reported functions of TNC include modulating macrophage polarization and improving MI BZ mechanics.<sup>5,35</sup> Using qPCR, we found that PDGF-AB-treated cFib had increased *TNC* gene expression as compared to TGF- $\beta$ 1-treated cFib controls (Figure 2H). This suggests that PDGF-AB treatment induces a unique ECM-synthesizing transcriptome compared to TGF- $\beta$ 1-mediated myofibroblast differentiation.

Next, we used our cFib RNAseq dataset to explore PDGF effects on other ECM-related genes. PDGF-AB-treated cFib differentially expressed 199 ECM-related genes, including multiple collagen subtypes, matrix metalloproteinases, a disintegrin and metalloproteinases with thrombospondin motifs (ADAMTS) and tissue inhibitors of metalloproteinases (TIMPs) (Figure 2I). Reactome, DAVID, and GSEA pathway analyses all showed that multiple pathways associated with ECM organization were both up- and downregulated in PDGF-AB-treated cFib (Figures 2D and 2I). ECM-related Reactome pathways upregulated in PDGF-AB-treated cFib included “degradation of the ECM, collagen degradation, collagen formation, collagen chain trimerization and ECM proteoglycans” (Figure 2J). Together these results show that PDGF-AB treatment of cFib unexpectedly reduces cell cycle pathways and induces a promigratory proangiogenic immunomodulatory cFib phenotype with unique modulation of the ECM that is distinct from cardiac myofibroblasts.

**PDGF-AB REDUCES MYOFIBROBLAST DIFFERENTIATION AND INCREASES CELL-CELL INTERACTIONS WITHIN INFARCT SCAR.** To assess how PDGF-AB impacts post-MI scar formation at the end of the proliferative phase (day 5), we administered PDGF-AB via osmotic minipump in a murine model of MI (Figure 3A). We then used IMC to assess different cell populations and their spatial interactions (Figure 3B).<sup>36</sup> To identify regions of interest in our tissues, we used a

combination of immunohistochemistry (IHC) from adjacent sections with a brightfield panorama generated on a Hyperion IMC imaging system (Supplemental Figures 7B and 7B). This allowed remote zone (RZ), BZ, and IZ regions of interest to be accurately selected during IMC data acquisition (Supplemental Figure 7). With images from our 24-antibody panel, we used a machine-learning multi-cut cell segmentation methodology that successfully segmented CMs from non-CMs and identified acellular regions (Supplemental Figures 8 to 10). Initial IMC cellular analyses revealed a decreased percentage of  $\alpha$ -SMA<sup>+</sup> and  $\alpha$ -SMA<sup>+</sup>Col1- $\alpha$ 1<sup>+</sup> cells (Figures 3C and 3D) within the IZ of PDGF-AB-treated mice, suggesting that PDGF-AB reduces fibroblast-myofibroblast differentiation post-MI.

Using t-distributed stochastic neighbor analyses to perform unbiased clustering, we show 19 distinct cell subtypes, each with distinct cell marker expression, including 4 CM, 5 fibroblast, and 3 myofibroblast subtypes (Figures 3E and 3F). One fibroblast subtype, with a vimentin<sup>+</sup>fibronectin<sup>+</sup>Ki67<sup>+</sup>Col1- $\alpha$ 1<sup>neg</sup> marker signature (named fibroblast 1) was significantly reduced in PDGF-AB IZs (Figures 3E to 3H). Because fibronectin and Ki67 are markers of fibroblasts in the post-MI proliferation phase, these data may suggest that PDGF-AB reduces fibroblast transition into a specific proliferative fibroblast subpopulation within the post-MI IZ.<sup>5</sup>

To elucidate PDGF-AB effects on cell-cell interactions, we then performed IMC spatial analyses for each cell subtype derived from unbiased clustering. We found a significant reduction in the average distance between multiple cell subtypes within the IZ of PDGF-AB-treated mice, without a significant difference in their proportions (Figure 3H, Supplemental Table 1). For example, within PDGF-AB IZs, the fibroblast 5 cell subtype showed a significantly reduced average distance from fibroblast 5, immune 1, fibroblast 3, CM 3, and cluster 16 cell subtypes, without any significant difference in their individual proportions (Figures 3H and 3I, Supplemental Table 1). These data suggest that PDGF-AB increases fibroblast interactions with other cardiac cells within the infarcted heart, possibly indicative of increased fibroblast migration.

**PDGF-AB REDUCES FIBROBLAST-MYOFIBROBLAST DIFFERENTIATION AND DOES NOT INCREASE PROLIFERATION IN A PIG MODEL OF MI.** To assess how PDGF-AB impacts post-MI scar remodeling in a clinically relevant large animal model, we used our established pig model of myocardial ischemia-

reperfusion with PDGF-AB systemic infusion (Figure 4A).<sup>17</sup> Pigs were subjected to 90-minute balloon occlusion of the left anterior descending (LAD) artery (Figure 4B, arrowhead) followed by reperfusion and osmotic minipump insertion. Cardiac magnetic resonance imaging (cMRI) was performed at both 2 and 9 days post-MI, whereas IHC and RNAseq were performed on pigs sacrificed 11 days post-MI (control n = 3, PDGF-AB-treated n = 3) (Figure 4A). IHC was also performed on pigs sacrificed 28 days post-MI using tissue from our previous PDGF-AB study.<sup>17</sup> Late gadolinium enhancement combined with cMRI analysis confirmed infarct creation with LVEF <45% (typical healthy porcine LVEF ~60% (Figures 4C and 4D, Supplemental Figure 11, Videos 4 and 5).<sup>37</sup> Although we have previously shown that PDGF-AB significantly increased LVEF 28 days post-MI, cMRI at the earlier timepoint of 9 days post-MI showed a nonstatistically significant trend towards improvement in the small number of animals in the current study (Figure 4D).<sup>16</sup> This may suggest that PDGF-AB has beneficial therapeutic effects as early as 9 days post-MI.

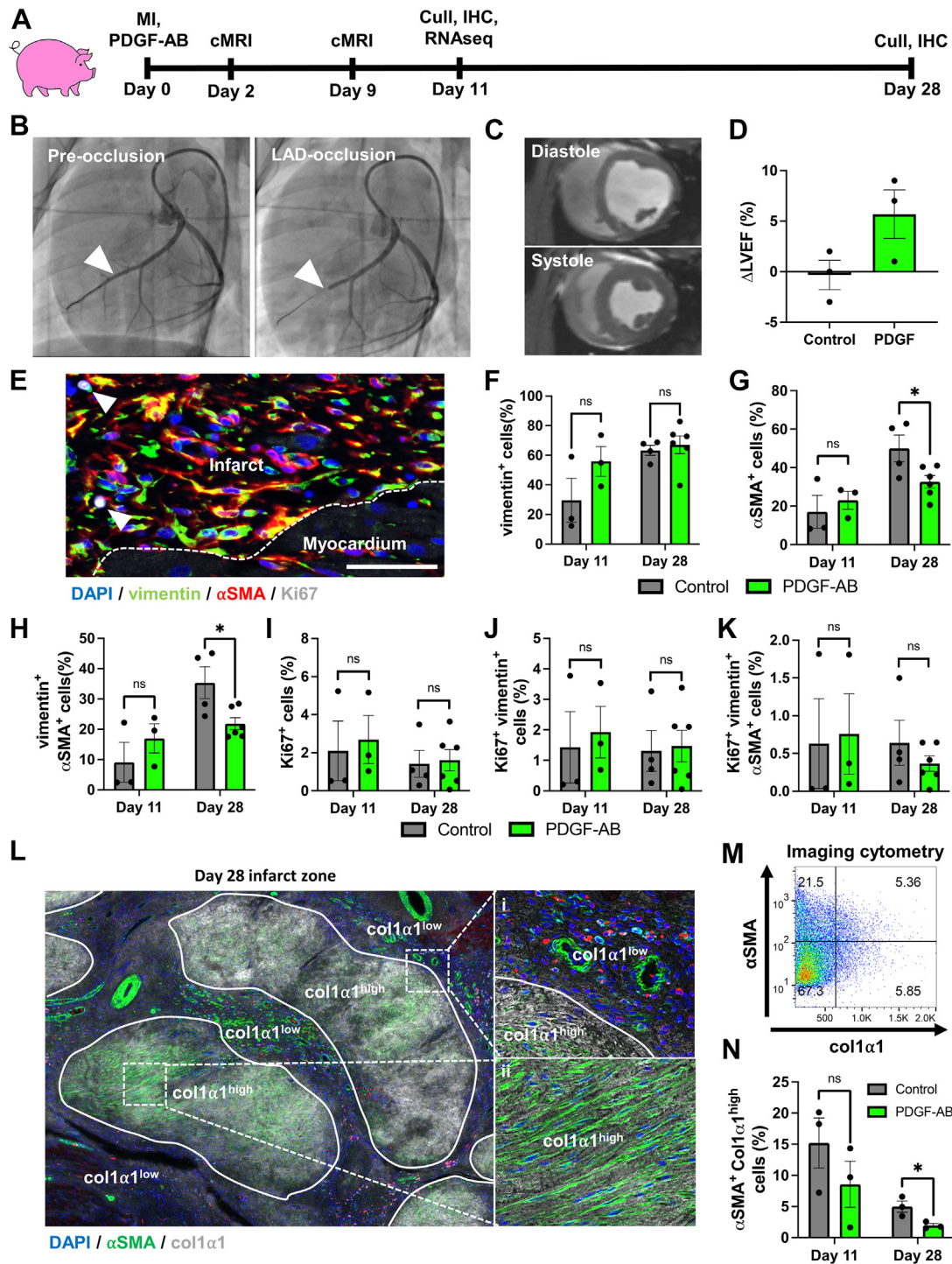
To assess whether PDGF-AB-treated pigs exhibited a similar reduction in fibroblast-myofibroblast differentiation observed in the in vitro and rodent experiments described above, we performed IHC analyses of the IZs. IHC analyses showed no difference in vimentin<sup>+</sup> fibroblast proportions at day 11 or day 28 (Figures 4E and 4F). Agreeing with in vitro cFib experiments described above, at day 28 we observed a significant decrease in both  $\alpha$ -SMA<sup>+</sup> cells and  $\alpha$ -SMA<sup>+</sup> vimentin<sup>+</sup> myofibroblasts and no significant difference in Ki67 cellular expression within IZ of PDGF-AB-treated pigs (Figures 4G to 4K). Further IHC analyses showed that PDGF-AB-treated pigs had a decreased number of  $\alpha$ SMA<sup>+</sup> cells with myofibroblast morphology in distinct col1- $\alpha$ 1<sup>high</sup> areas of IZs at day 28 (Figures 4L to 4N). Together, these results show that PDGF-AB reduces fibroblast-myofibroblast differentiation in post-MI pigs while having no detectable effect on proliferation.

**DE NOVO TRANSCRIPTOME ASSEMBLY IMPROVES UPON THE CURRENT SSCROFA11.1 PIG REFERENCE GENOME.** For a further understanding of PDGF-AB effects post-MI, we performed deep (>10<sup>7</sup> reads/sample) paired-end RNAseq on pig post-MI cardiac tissue. Combining this with de novo transcriptome assembly provided an opportunity to improve upon the current pig reference genome annotation Sscrofa11.1.<sup>19</sup> Although Sscrofa11.1 and its associated annotations have been an important advancement,





**FIGURE 4** PDGF-AB Reduces Fibroblast-Myofibroblast Differentiation and Does Not Increase Proliferation in Pigs Post-MI



**(A)** Schematic of post-MI pig model. **(B)** Coronary angiogram pre- and post-left anterior descending (LAD) artery balloon occlusion to induce MI. Arrowhead indicates balloon inflation point in LAD. **(C)** Short-axis cMRI view of the heart in end-diastole and end-systole at the mid-papillary muscle level. **(D)** Change in left ventricular ejection fraction ( $\Delta$ LVEF) from day 2 to day 9 post-MI. **(E to K)** Immunohistochemistry (IHC) and analyses for fibroblasts (vimentin<sup>+</sup>), myofibroblasts (vimentin<sup>+</sup> $\alpha$ SMA<sup>+</sup>) and proliferating (Ki67<sup>+</sup>) cells within pig post-MI IZ (scale bar = 100  $\mu$ m). **(L to N)** IHC and analyses of  $\alpha$ SMA<sup>+</sup> cells with myofibroblast morphology within col1 $\alpha$ 1<sup>high</sup> areas in pig IZs. cMRI = cardiac magnetic resonance imaging; other abbreviations as in Figures 1 and 3.

they are still far from complete.<sup>19</sup> Using de novo assembly, we improved from 27,091 (Sscrofa11.1) to 41,627 (de novo) genes and from 114,292 (Sscrofa11.1) to 356,721 (de novo) transcripts, thus significantly expanding the current annotations of the pig genome (Figures 5A and 5B). This provides an important resource for the scientific community to investigate the pig cardiac transcriptome.

**PDGF AND MATRIX MODULATION PATHWAYS ARE HIGHLIGHTED IN EARLY MYOCARDIAL INFARCT REPAIR IN UNTREATED PIGS.** We next used the de novo transcriptome assembly to investigate novel genes, transcription factors, and lncRNA associated with pathophysiological changes after MI. We compared control (untreated) infarcted pigs to sham (noninfarcted) pigs and identified differential expression of >1,500 known and >1,000 novel transcripts in the IZ, BZ, RZ, and right ventricles of pigs 11 days post-MI (Figures 5C and 5D, Supplemental Figure 12A). Here “known” denotes pig genes previously annotated but not necessarily described as differentially expressed post-MI. Strikingly, analysis using DAVID and GSEA revealed “PDGF growth factor binding” and “signaling by PDGF” were among upregulated pathways in control (untreated) infarcted cardiac tissue (Figure 5E, Supplemental Figure 12B). This shows that PDGF-related genes are pathophysiologically upregulated 11 days after MI in pigs and highlights the importance of PDGF signaling in response to the cardiac repair process. GSEA also showed that 8 of 10 of the top upregulated Reactome gene sets were ECM-related (Figure 5E). These gene sets included “ECM organization, ECM proteoglycans, degradation of the ECM, collagen degradation, and collagen chain trimerization” (Figure 5E) and were the same gene sets upregulated in in vitro experiments on PDGF-AB-treated human cFib described in Figure 2J. Together, these data suggest that PDGF-mediated pathways and ECM pathways that overlap with PDGF-treated cFib are critically involved in the postinfarct cardiac milieu.

**PDGF-AB ACCELERATES EARLY SCAR MATURATION AND REDUCES INFLAMMATORY CYTOKINE GENE EXPRESSION IN A PIG MODEL OF MI.** Increased post-MI scar anisotropy (directionality) is associated with improved heart function and scar maturity.<sup>38,39</sup> We have previously shown that PDGF-AB increases pig scar anisotropy 28 days post-MI.<sup>17</sup> Therefore, we investigated how PDGF-AB impacts scar remodeling 11 days post-MI. Using our de novo library assembly and pig RNAseq dataset, we performed DE analysis of

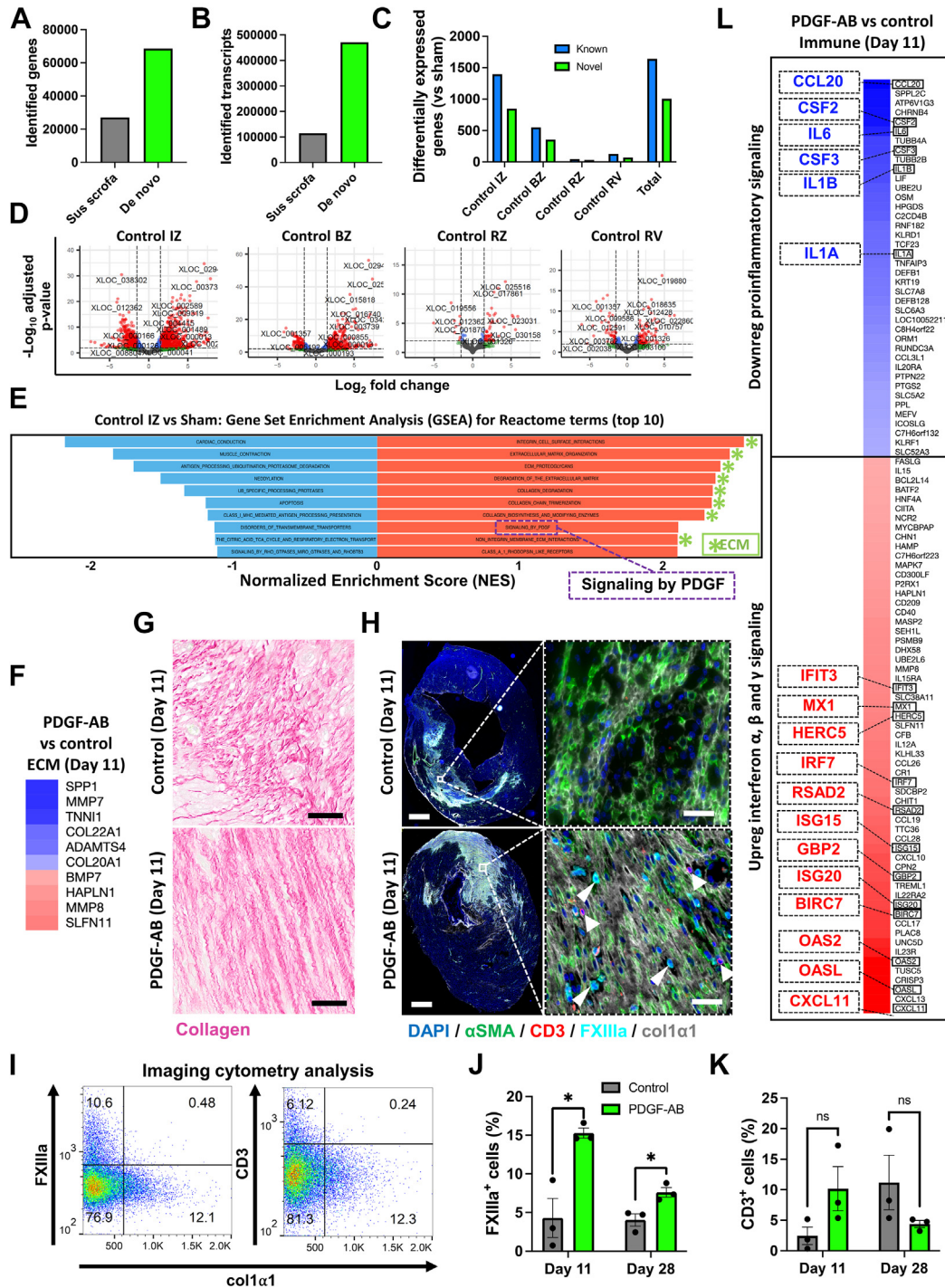
day 11 PDGF-AB-treated pigs compared to infarcted untreated controls. PDGF-AB-treated pigs showed both up- and downregulation of ECM-related genes including collagens and matrix metalloproteinases (Figure 5F). Using Picro-Sirius Red histological collagen staining, we also show that PDGF-AB increased scar anisotropy at this earlier timepoint, similar to that observed at 28 days post-MI in our previous study (Figure 5G).<sup>17</sup>

To further understand the effects of PDGF-AB on ECM organization and the immune response, we performed IHC on PDGF-treated pigs, specifically probing for expression of  $\alpha$ SMA, CD3 (T cells), FXIIIa (M2 anti-inflammatory/proreparative macrophages), and col1 $\alpha$ 1 (fibrotic scar).<sup>40</sup> PDGF-AB-treated pig IZs showed  $\alpha$ SMA<sup>+</sup> cells aligned in a homogeneous and anisotropic col1 $\alpha$ 1 scar (Figure 5H, Supplemental Figures 13 and 14). Conversely, in control pig IZs, we found  $\alpha$ SMA<sup>+</sup> cells within more heterogeneous and less organized col1 $\alpha$ 1 scar (Figure 5H, Supplemental Figures 13 and 14). As it is known that scar col1 $\alpha$ 1 content and anisotropy increase with post-MI scar maturity in large animal models, our data therefore suggest that PDGF-AB accelerates scar maturation.<sup>39</sup> PDGF-AB also increased FXIIIa<sup>+</sup> cells within the IZ at both day 11 and day 28 (Figures 5H to 5J, Supplemental Figures 13 and 14), indicating an increase in reparative anti-inflammatory M2 macrophages. We also observed a nonsignificant trend of increased CD3<sup>+</sup> T cells at day 11 in PDGF-AB-treated pigs which reversed at day 28 (Figures 5H to 5J, Supplemental Figures 13 and 14).

Increased or prolonged post-MI expression of proinflammatory cytokines such as interleukin (IL)-1 and IL-6 is associated with poor clinical outcomes, with inhibition of this process being explored in clinical trials.<sup>7-10</sup> Using DE analysis of immune response genes (Reactome-curated gene set) our data show that PDGF-AB-treated pigs downregulate proinflammatory cytokines IL-1A, IL-1B, IL-6, colony-stimulating factor (CSF)-2 (also known as granulocyte-macrophage colony-stimulating factor), and CSF-3 (also known as granulocyte colony-stimulating factor) (Figure 5L). Additionally, DE analysis showed that PDGF-AB induced upregulation of genes associated with interferon signaling (Figure 5L). These data show that PDGF-AB alters the pig infarct immune response by reducing proinflammatory cytokines and upregulating interferon signaling. Together, these data suggest that PDGF-AB reduces inflammation and accelerates scar maturation after MI.



**FIGURE 5** De Novo Genome Assembly Reveals Novel Pig Genes, Transcripts, and Infarct Biology and Shows That PDGF-AB Accelerates Scar Maturation and Reduces Inflammatory Cytokines in Pigs Post-MI



(A, B) Number of identified genes and transcripts for current pig genome annotation (SScrofa11.1) and our de novo library assembly. (C) DE genes for control pig 11 days post-MI cardiac tissue vs shams using our de novo library assembly. (D) DE genes for control pigs (vs shams). Red dots represent genes that met both *P* value and  $\log_2$ (fold change) cutoffs. (E) GSEA for control DE genes in control pigs (vs shams). (F) Heatmap of PDGF-AB-treated pig RNAseq for DE ECM-related genes. (G) Picro-Sirius red histological staining of collagen fibers (red) in pig post-MI infarct zone (IZ, scale bar = 50  $\mu$ m). (H) IHC of col1 $\alpha$ 1 scar (grey), CD3<sup>+</sup> T cells (red, arrows), and FXIIIa<sup>+</sup> macrophages (blue, arrowheads) in pigs post-MI. Scale bar = 2 mm (top) and 100  $\mu$ m (bottom). (I to K) IHC image analyses of pig infarct zones (\**P* < 0.05). (L) Heatmap of PDGF-AB-treated pig RNAseq for DE immune-related genes. Abbreviations as in Figures 1 to 4.



**PDGF-AB AFFECTS TRANSCRIPT VARIANT AND lncRNA EXPRESSION WITHIN CELL CYCLE AND TGF- $\beta$  PATHWAYS IN PIGS POST-MI.** To understand whether PDGF-AB impacts alternative RNA splicing and therefore produced different transcript variants, we performed differential transcript usage (DTU) analysis using our de novo transcriptome assembly. DTU quantifies the proportion of each transcript variant for each gene and determines if this proportion was significantly affected. Within pig, infarcted tissue DTU of immune response genes such as *CSFR1* and cell cycle genes such as cyclin-T1 (*CCNT1*) and aurora B kinase (*AURKB*), varied in PDGF-AB compared to control treated pigs (Supplemental Figures 15A to 15C). DAVID analysis comparing both control and PDGF-AB-treated pigs to shams revealed a range of pathways with DTU (Supplemental Figure 15D). Within these pathways, some were uniquely altered by PDGF-AB, such as angiogenesis in the BZ and mitosis and cell division in the IZ (Supplemental Figure 15D). Notably, signal transduction pathways effected by DTU included TGF- $\beta$  signaling pathways that are responsible for fibroblast-myofibroblast differentiation (Supplemental Figure 15E).<sup>41</sup> In total, >600 genes showed DTU in PDGF-AB compared to controls (Supplemental Figure 15F). Reactome analyses comparing PDGF-AB-treated pig IZs to control IZs revealed DTU in cell cycle, immune system, and signal transduction pathways (Supplemental Figure 15G).

Further complexity in the transcriptome is introduced when considering lncRNAs; RNAs longer than 200 nucleotides that are not translated into functional proteins.<sup>42</sup> Instead, lncRNAs can affect expression of nearby genes by impacting their transcription and can have significant implications during post-MI remodeling.<sup>42,43</sup> Using our de novo library assembly, we identified 96 downregulated and 77 upregulated novel lncRNAs that were differentially expressed in PDGF-AB-treated pigs (Supplemental Figure 16A). By identifying genes proximal to lncRNAs, we could predict which genes they effect. Combining this method with Gene Ontology term analysis revealed that PDGF-AB induces downregulation of lncRNAs proximal to genes associated with cell cycle, ECM degradation, and interferon-I signaling pathways (Supplemental Figure 16B). PDGF-AB upregulates lncRNAs proximal to genes associated with migration, angiogenesis, and again interferon-I signaling (4 of 10 top upregulated pathways) (Supplemental Figures 16B and 17). Together these data suggest PDGF-AB also affects myofibroblast differentiation, cell cycle, migration, ECM synthesis, angiogenesis, and immune response

post-MI through alternative splicing and lncRNA expression.

## DISCUSSION

In our previous pig study, we showed that PDGF-AB improved heart function.<sup>17</sup> We also showed that PDGF-AB increased collagen scar alignment and homogeneity 28 days post-MI.<sup>17</sup> These are both signs of successful reparative scar modulation in contrast to the disorganized scar and adverse remodeling that usually follows MI.<sup>39</sup> In the current study, we again show these findings 11 days post-MI in a clinically relevant porcine model. Because fibroblasts respond to MI by undergoing sequential phenotypic changes integral to scar formation, we hypothesized that PDGF-AB alters fibroblast phenotype to facilitate beneficial infarct remodeling.<sup>3-5</sup> Using human, mouse, and pig models we here show that PDGF-AB reduces myofibroblast differentiation, alters ECM synthesis, and increases migration without increasing proliferation. These unique effects of PDGF-AB provide further understanding into its beneficial therapeutic efficacy and may provide insight for other antifibrotic therapies.<sup>44</sup>

Previous studies report that PDGFs increase fibrosis by induction of fibroblast-myofibroblast differentiation.<sup>13-15</sup> However, we have previously shown in multiple models that PDGF-AB does not increase cardiac fibrosis post-MI.<sup>16-18</sup> In this study, we assessed the effects of PDGFs on cardiac fibroblast-myofibroblast differentiation in models using multiple species. Unexpectedly, we found that PDGF-AB reduced myofibroblast differentiation both in vitro (Figure 1) and post-MI (Figures 3 and 4) and effected alternative splicing of genes within TGF- $\beta$  signaling pathways (Supplementary Figure 15). Although further studies are required to elucidate the underlying mechanism of PDGF-AB, these data raise the possibility that PDGF-AB is driving cardiac fibroblasts into a unique phenotype that is distinct from myofibroblasts. Interestingly, lineage reporter studies show myofibroblast states are both unstable and reversible, governed by *MBLN1* and its stabilization of *SRF*.<sup>25,31,32</sup> In our study, we show that PDGF-AB reduces *ACTA2*, *MBLN1*, and *SRF* and other myofibroblast markers compared to both untreated and TGF- $\beta$ 1 controls (Figure 1). This suggests that PDGF-AB induces dedifferentiation of cFib from a cardiac myofibroblast state. Our live cell imaging also supports this hypothesis, showing cFib progression from a wide-flat to spindle-shaped morphology following PDGF-AB treatment (Video 2). If confirmed in vivo using future lineage tracing studies, the ability of PDGF-AB

to dedifferentiate myofibroblasts could increase its therapeutic potential. For instance, PDGF-AB could be used to target both fibroblast and myofibroblast populations during late-stage infarct remodeling and fibrotic events in other organs. To this point, a limitation of the study is the absence of fibroblast-specific *in vivo* approaches to specifically document the role of PDGF's reparative actions; this should be explored in future studies.

Supporting our findings, a study by Juhl et al<sup>14</sup> used qPCR and histology to show that PDGF treatment induces a unique ECM profile compared to TGF- $\beta$ 1-induced myofibroblast differentiation in dermal fibroblasts. In our study, we confirm these findings in human cFib using RNAseq to show that PDGF-AB-treated cFib express a unique ECM transcriptome distinct from myofibroblasts (Figure 3). These data show the unique effects of PDGF-AB on cardiac fibroblasts. Further research into the underappreciated heterogeneity of cardiac fibroblasts is needed and may lead to new therapies for infarct remodeling.

Perhaps a hesitancy to use PDGF-AB as a clinical therapy may arise from previous studies reporting PDGFs to be fibroblast mitogens.<sup>11</sup> If this were to be the case, then *in vivo* delivery of PDGFs would increase scar size post-MI. However, all of our previous studies have shown that PDGF-AB does not increase post-MI scar size.<sup>16-18</sup> Therefore, we investigated proliferation in all of our animal models to understand the mitogenic potential of PDGFs post-MI. In our models, we show that PDGF-AB: 1) reduces cell cycle pathways in cFib; 2) depletes a specific mouse proliferation phase fibroblast population (vimentin<sup>+</sup>fibronectin<sup>+</sup>Ki67<sup>+</sup>Col1- $\alpha$ 1<sup>neg</sup>) post-MI; 3) has no effect on fibroblast or myofibroblast proliferation in post-MI pigs; 4) induces alternative splicing of cell cycle genes; and 5) downregulates lncRNAs proximal to cell cycle genes (Figures 2, 4, and 5, Supplemental Figures 15 and 16). Although these results contrast with some prior reports, other studies support our findings that PDGFs do not necessarily induce proliferation. Kim et al<sup>45</sup> have shown that PDGFs induce migration but not proliferation in osteoblastic cells. Furthermore, De Donatis et al<sup>46</sup> show in a mouse fibroblast cell line that PDGFs induce either migration or proliferation depending on dosage. Although it remains possible that doses higher than what we have used *in vivo* can influence proliferation, the dosages used in our previous studies have shown therapeutic efficacy in both small and large animal models.<sup>16-18</sup>

In our current and previous studies, we show that PDGF-AB treatment increases scar anisotropy (directionality) post-MI.<sup>17</sup> Possible explanations for this

anisotropy may be altered fibroblast fate and phenotype with associated differences in ECM-related gene expression. For example, we show that PDGF-AB-treated cFib undergo reduced myofibroblast differentiation (Figure 1) and distinct gene expression related to ECM synthesis and degradation (Figure 2). This includes genes integral to scar formation such as *COL1A1*, *COL1A2*, and *LOX* (Figure 2). However, future fibroblast fate mapping studies, single-cell RNAseq, and proteomic assessment of the scar are required to confirm these hypotheses.

Prolonged or excessive post-MI expression of proinflammatory cytokines, such as IL-1 and IL-6, is associated with adverse remodeling and decreased heart function.<sup>7,8</sup> Current clinical trials to block these cytokines indicate potential to reduce post-MI heart failure.<sup>9,10</sup> Moreover, Jing et al<sup>48</sup> have previously shown that IL-6 knockout mice increase their ratio of anti-inflammatory (M2) to proinflammatory (M1) macrophages, thus favoring a reparative phenotype and improved heart function.<sup>47,48</sup> We have previously shown that post-MI PDGF-AB treatment in mice increased the M2:M1 macrophage ratio.<sup>18</sup> In this study we show that PDGF-AB both reduces proinflammatory cytokines (eg, IL-1 and IL-6) and increases pro-reparative M2 macrophages in pigs (Figure 5). As reduced inflammation and increased M2 macrophages improve heart function and are hallmarks of the scar maturation phase, this provides a further understanding into the beneficial effects of PDGF-AB treatment post-MI.<sup>5</sup>

PDGFs have been shown to induce angiogenesis<sup>49</sup> and we have previously shown that this occurs following PDGF-AB-treatment in a pig model of MI.<sup>17</sup> As others have shown that PDGFs induce proliferation and migration of vascular cells,<sup>49</sup> it may be predicted that this would be the source of angiogenesis during post-MI PDGF treatment. However, in our study, we also show that PDGFs induced a proangiogenic fibroblast phenotype in human cardiac fibroblasts, suggesting an additional source of angiogenesis. Furthermore, we show that PDGF-AB treatment in pigs induced alternative splicing of genes associated with angiogenesis in the border zone and increased expression of lncRNAs with predicted targets of genes in angiogenic pathways. Together, these findings are of significance because of their potential to reduce the damaging effects of ischemia through formation of neovessels within and around the infarct.

Post-MI scar formation is essential to replace necrotic tissue. An effective reparative process requires enough collagenous scar formation to prevent cardiac rupture, while simultaneously avoiding

prolonged excessive fibrosis which can reduce heart function. Despite previous studies showing fibrogenic effects of PDGFs in organs other than the heart,<sup>50,51</sup> previous work by our group has shown either no increase or a decrease in post-MI scar size/fibrosis.<sup>16,17</sup> Our work supports the hypothesis that quantity of scar does not need to be reduced to improve post-MI cardiac function, but instead quality and composition of scar formation altered. For example, in the current study, we show that PDGF-treated cFib has a unique, altered, but not decreased ECM-related genomic profile. Furthermore, our pig studies also show altered (anisotropic) scar formation but no effect on scar size.<sup>17</sup> Overall, this suggests that a more nuanced therapeutic approach may be beneficial: improve scar organization and its ECM constituents, rather than aiming only to reduce scar size.

**STUDY LIMITATIONS.** We acknowledge that a limitation of the current study is the use of different post-MI timepoints for mouse and pig tissue collection that reduces direct comparisons between the models. That said, using 2 timepoints has permitted the investigation of PDGF-AB effects at different stages of infarct resolution.

## CONCLUSIONS

Here we show that PDGF-AB treatment after MI reduces cardiac fibroblast-myofibroblast differentiation and induces a distinct fibroblast phenotype without increased proliferation. This highlights PDGF-AB's pleiotropic effects and challenges the concept that PDGFs are exclusively fibroblast mitogens or fibrotic growth factors. Combined with our previous studies, we reveal further understanding into PDGF-AB's beneficial effects after MI and provide compelling evidence for its clinical translation.<sup>16-18</sup> Because the effects of PDGFs post-MI contrast conventional anti-fibrotic strategies, this study may provide new ground for future drug discovery research.<sup>44</sup>

**ACKNOWLEDGMENTS** The authors thank Sheryl Foster for assistance with cMRI; Juntang Lu, Vu Tran, Lachlan Pearson, and Tony Barry for pig animal care; and Sydney Cytometry Core Research Facility, a joint initiative of Centenary Institute and the University of

Sydney, for assistance with Imaging Mass Cytometry. Image acquisition and analysis were performed at Westmead Imaging Facility which is supported by the Westmead Institute for Medical Research and the National Health and Medical Research Council.

## FUNDING SUPPORT AND AUTHOR DISCLOSURES

This study was funded by grants from the National Health and Medical Research Council APP1194139 and from the New South Wales Government Office of Health and Medical Research. HAYA scientific provided funding for paired-end RNAseq of pig cardiac tissue. Drs Marcuello, Blessing, and Ounzain are shareholders and full-time employees of HAYA therapeutics. All other authors have reported that they have no relationships relevant to the contents of this paper to disclose.

**ADDRESS FOR CORRESPONDENCE:** Dr James J.H. Chong, Westmead Institute for Medical Research, 176 Hawkesbury Road, Westmead, New South Wales 2145, Australia. E-mail: [james.chong@sydney.edu.au](mailto:james.chong@sydney.edu.au). Twitter: [@jameschong\\_doc](https://twitter.com/jameschong_doc).

## PERSPECTIVES

**COMPETENCY IN MEDICAL KNOWLEDGE:** We have previously shown that systemic infusion of human recombinant PDGF-AB into a clinically relevant pig model improves heart function and effects fibrotic scar formation 28 days following MI. With potential clinical trials in the near future, understanding how these effects manifest in early infarct repair is required. Using human, mouse and clinically relevant pig models, we investigated how PDGF-AB affects the post-MI cellular and transcriptome environments. We reveal that PDGF-AB impacts the fibrotic process without increasing fibroblast proliferation.

**TRANSLATIONAL OUTLOOK:** Understanding these beneficial effects on the post-MI environment strengthens the case for clinical translation of PDGF-AB. Additionally, by understanding how PDGF-AB beneficially alters infarct scar formation may present potential new strategies for treating MI, thus helping the development of novel therapeutics.

## REFERENCES

- Virani SS, Alonso A, Benjamin EJ, et al. Heart disease and stroke statistics-2020 update: a report from the American Heart Association. *Circulation*. 2020;141(9):E139–E596.
- Palasubramaniam J, Wang X, Peter K. Myocardial infarction – from atherosclerosis to thrombosis. *Arterioscler Thromb Vasc Biol*. 2019;39(8):E176–E185.
- Hume RD, Chong JJH. The cardiac injury immune response as a target for regenerative and cellular therapies. *Clin Ther*. 2020;42(10):1923–1943.
- Mouton AJ, Ma Y, Rivera Gonzalez OJ, et al. Fibroblast polarization over the myocardial infarction time continuum shifts roles from inflammation to angiogenesis. *Basic Res Cardiol*. 2019;114(2):6.
- Silva AC, Pereira C, Fonseca ACRG, Pinto-do-Ó P, Nascimento DS. Bearing my heart: the role of extracellular matrix on cardiac development, homeostasis, and injury response. *Front Cell Dev Biol*. 2021;8:621644.
- Nakaya M, Watari K, Tajima M, et al. Cardiac myofibroblast engulfment of dead cells facilitates recovery after myocardial infarction. *J Clin Invest*. 2017;127(1):383.
- Abbate A, Toldo S, Marchetti C, Kron J, Van Tassell BW, Dinarello CA. Interleukin-1 and the inflammasome as therapeutic targets in cardiovascular disease. *Circ Res*. 2020;126(9):1260–1280.
- Groot HE, Al Ali L, van der Horst ICC, et al. Plasma interleukin 6 levels are associated with cardiac function after ST-elevation myocardial infarction. *Clin Res Cardiol*. 2019;108(6):612.
- Buckley LF, Abbate A. Interleukin-1 blockade in cardiovascular diseases: from bench to bedside. *BioDrugs*. 2018;32(2):111–118.
- Abbate A, Trankle CR, Buckley LF, et al. Interleukin-1 blockade inhibits the acute inflammatory response in patients with ST-segment-elevation myocardial infarction. *J Am Heart Assoc*. 2020;9(5):e01494.
- Papadopoulos N, Lennartsson J. The PDGF/PDGR pathway as a drug target. *Mol Aspects Med*. 2018;62:75–88.
- Chen PH, Chen X, He X. Platelet-derived growth factors and their receptors: structural and functional perspectives. *Biochim Biophys Acta*. 2013;1834(10):2176.
- Singh V, Barbosa FL, Torricelli AAM, Santhiago MR, Wilson SE. Transforming growth factor  $\beta$  and platelet-derived growth factor modulation of myofibroblast development from corneal fibroblasts in vitro. *Exp Eye Res*. 2014;120:152–160.
- Juhl P, Bondesen S, Hawkins CL, et al. Dermal fibroblasts have different extracellular matrix profiles induced by TGF- $\beta$ , PDGF and IL-6 in a model for skin fibrosis. *Sci Rep*. 2020;10(1):17300.
- Leask A. Potential therapeutic targets for cardiac fibrosis: TGF $\beta$ , angiotensin, endothelin, CCN2, and PDGF, partners in fibroblast activation. *Circ Res*. 2010;106(11):1675–1680.
- Rashid FN, Clayton ZE, Ogawa M, et al. Platelet derived growth factor-A (Pdgf-a) gene transfer modulates scar composition and improves left ventricular function after myocardial infarction. *Int J Cardiol*. 2021;341:24–30.
- Thavapalachandran S, Grieve SM, Hume RD, et al. Platelet-derived growth factor-AB improves scar mechanics and vascularity after myocardial infarction. *Sci Transl Med*. 2020;12(524):eaay2140.
- Asli NS, Xaymardan M, Forte E, et al. PDGFR $\alpha$  signaling in cardiac fibroblasts modulates quiescence, metabolism and self-renewal, and promotes anatomical and functional repair. *bioRxiv*. 2018:225979.
- Warr A, Affara N, Aken B, et al. An improved pig reference genome sequence to enable pig genetics and genomics research. *Gigascience*. 2020;9(6):giaa051.
- Broad Institute. MORPHEUS Versatile matrix visualization and analysis software. Accessed May 19, 2023. <https://software.broadinstitute.org/morpheus/>
- Yousefi F, Shabaninejad Z, Vakili S, et al. TGF- $\beta$  and WNT signaling pathways in cardiac fibrosis: non-coding RNAs come into focus. *Cell Commun Signal*. 2020;18(1):87.
- Chong JJH, Chandrakanthan V, Xaymardan M, et al. Adult cardiac-resident MSC-like stem cells with a proepicardial origin. *Cell Stem Cell*. 2011;9(6):527–540.
- Gabasa M, Royo D, Molina-Molina M, et al. Lung myofibroblasts are characterized by down-regulated cyclooxygenase-2 and its main metabolite, prostaglandin E2. *PLoS One*. 2013;8(6):e65445.
- Weder B, Mamie C, Rogler G, et al. BCL2 regulates differentiation of intestinal fibroblasts. *Inflamm Bowel Dis*. 2018;24(9):1953–1966.
- Kanasicak O, Khalil H, Ivey MJ, et al. Genetic lineage tracing defines myofibroblast origin and function in the injured heart. *Nat Commun*. 2016;7:12260.
- Gibb AA, Lazaropoulos MP, Elrod JW. Myofibroblasts and fibrosis: mitochondrial and metabolic control of cellular differentiation. *Circ Res*. 2020;127(3):427–447.
- Torr EE, Ngam CR, Bernau K, Tomasini-Johansson B, Acton B, Sandbo N. Myofibroblasts exhibit enhanced fibronectin assembly that is intrinsic to their contractile phenotype. *J Biol Chem*. 2015;290(11):6951.
- Kishimoto Y, Kishimoto AO, Ye S, Kendziorski C, Welham NV. Modeling fibrosis using fibroblasts isolated from scarred rat vocal folds. *Lab Invest*. 2016;96(7):807–816.
- Fu X, Khalil H, Kanasicak O, et al. Specialized fibroblast differentiated states underlie scar formation in the infarcted mouse heart. *J Clin Invest*. 2018;128(5):2127–2143.
- Zhang Z, Nie F, Chen X, et al. Upregulated periostin promotes angiogenesis in keloids through activation of the ERK 1/2 and focal adhesion kinase pathways, as well as the upregulated expression of VEGF and angiopoietin-1. *Mol Med Rep*. 2015;11(2):857–864.
- Davis J, Salomonis N, Ghearing N, et al. MBNL1-mediated regulation of differentiation RNAs promotes myofibroblast transformation and the fibrotic response. *Nat Commun*. 2015;6(1):1–14.
- Bugg D, Bailey LRJ, Bretherton RC, et al. MBNL1 drives dynamic transitions between fibroblasts and myofibroblasts in cardiac wound healing. *Cell Stem Cell*. 2022;29(3):419–433.e10.
- Naomi R, Ridzuan PM, Bahari H. Current insights into collagen type I. *Polymers (Basel)*. 2021;13(16):2642.
- González-Santamaría J, Villalba M, Busnadiego O, et al. Matrix cross-linking lysyl oxidases are induced in response to myocardial infarction and promote cardiac dysfunction. *Cardiovasc Res*. 2016;109(1):67–78.
- Imanaka-Yoshida K, Tawara I, Yoshida T. Tenascin-C in cardiac disease: a sophisticated controller of inflammation, repair, and fibrosis. *Am J Physiol Cell Physiol*. 2020;319(5):C781–C796.
- Baharlou H, Canete NP, Cunningham AL, Harman AN, Patrick E. Mass cytometry imaging for the study of human diseases-applications and data analysis strategies. *Front Immunol*. 2019;10:2657.
- Charles CJ, Lee P, Li RR, et al. A porcine model of heart failure with preserved ejection fraction: magnetic resonance imaging and metabolic energetics. *ESC Heart Fail*. 2020;7(1):92–102.
- Voorhees AP, Han HC. A model to determine the effect of collagen fiber alignment on heart function post myocardial infarction. *Theor Biol Med Model*. 2014;11(1):6.
- Clarke SA, Richardson WJ, Holmes JW. Modifying the mechanics of healing infarcts: is better the enemy of good? *J Mol Cell Cardiol*. 2016;93:115.
- Töröcsik D, Bárdos H, Nagy L, Ádány R. Identification of factor XIII-A as a marker of alternative macrophage activation. *Cell Mol Life Sci*. 2005;62(18):2132–2139.
- Walton KL, Johnson KE, Harrison CA. Targeting TGF- $\beta$  mediated SMAD signaling for the prevention of fibrosis. *Front Pharmacol*. 2017;8:461.
- Statello L, Guo CJ, Chen LL, Huarte M. Gene regulation by long non-coding RNAs and its biological functions. *Nat Rev Mol Cell Biol*. 2021;22(2):96–118.



43. Micheletti R, Plaisance I, Abraham BJ, et al. The long noncoding RNA Wisper controls cardiac fibrosis and remodeling. *Sci Transl Med*. 2017;9(395):eaai9118.
44. Park S, Nguyen NB, Pezhouman A, Ardehali R. Cardiac fibrosis: potential therapeutic targets. *Transl Res*. 2019;209:121-137.
45. Kim SJ, Kim SY, Kwon CH, Kim YK. Differential effect of FGF and PDGF on cell proliferation and migration in osteoblastic cells. *Growth Factors*. 2007;25(2):77-86.
46. De Donatis A, Comito G, Buricchi F, et al. Proliferation versus migration in platelet-derived growth factor signaling. *J Biol Chem*. 2008;283(29):19948-19956.
47. Kim Y, Nurakhayev S, Nurkesh A, Zharkinbekov Z, Saparov A. Macrophage polarization in cardiac tissue repair following myocardial infarction. *Int J Mol Sci*. 2021;22(5):1-15.
48. Jing R, Long TY, Pan W, Li F, Xie QY. IL-6 knockout ameliorates myocardial remodeling after myocardial infarction by regulating activation of M2 macrophages and fibroblast cells. *Eur Rev Med Pharmacol Sci*. 2019;23(14):6283-6291.
49. Kalra K, Eberhard J, Farbehi N, Chong JJ, Xaymardan M. Role of PDGF-A/B ligands in cardiac repair after myocardial infarction. *Front Cell Dev Biol*. 2021;9:669188.
50. Iwayama T, Olson LE. Involvement of PDGF in fibrosis and scleroderma: recent insights from animal models and potential therapeutic opportunities. *Curr Rheumatol Rep*. 2013;15(2):304.
51. Klinkhammer BM, Floege J, Boor P. PDGF in organ fibrosis. *Mol Aspects Med*. 2018;62:44-62.

---

**KEY WORDS** myocardial infarction, platelet-derived growth factor

---

**APPENDIX** For supplemental tables, videos, figures, and text, please see the online version of this paper.